HUMAN GENE THERAPY 22:1143–1153 (September 2011)

DOI: 10.1089/hum.2010.245

Optimizing Promoters for Recombinant Adeno-Associated Virus-Mediated Gene Expression in the Peripheral and Central Nervous System Using Self-Complementary Vectors

Steven J. Gray,[1] Stacey B. Foti,[1] Joel W. Schwartz,[2,3] Lavanya Bachaboina,[1] Bonnie Taylor-Blake,[4] Jennifer Coleman,[4] Michael D. Ehlers,[2] Mark J. Zylka,[4] Thomas J. McCown,[1,5,6] and R. Jude Samulski[1,7]

Abstract

With the increased use of small self-complementary adeno-associated viral (AAV) vectors, the design of compact promoters becomes critical for packaging and expressing larger transgenes under ubiquitous or cell-specific control. In a comparative study of commonly used 800-bp cytomegalovirus (CMV) and chicken β-actin (CBA) promoters, we report significant differences in the patterns of cell-specific gene expression in the central and peripheral nervous systems. The CMV promoter provides high initial neural expression that diminishes over time. The CBA promoter displayed mostly ubiquitous and high neural expression, but substantially lower expression in motor neurons (MNs). We report the creation of a novel hybrid form of the CBA promoter (CBh) that provides robust long-term expression in all cells observed with CMV or CBA, including MNs. To develop a short neuronal promoter to package larger transgenes into AAV vectors, we also found that a 229-bp fragment of the mouse methyl-CpG-binding protein-2 (MeCP2) promoter was able to drive neuron-specific expression within the CNS. Thus the 800-bp CBh promoter provides strong, long-term, and ubiquitous CNS expression whereas the MeCP2 promoter allows an extra 570-bp packaging capacity, with low and mostly neuronal expression within the CNS, similar to the MeCP2 transcription factor.

Introduction

Adeno-associated viral (AAV) vectors have been used in research, preclinical, and clinical gene delivery studies primarily because these vectors transduce nondividing cells and confer long-term stable gene expression without associated inflammation or toxicity (Haberman *et al.*, 1998; Bessis *et al.*, 2004; Goncalves, 2005). AAV has a single-stranded 4.7-kb genome, and after removal of 4.4 kb of the viral genome recombinant vectors can be packaged with a similar-sized foreign piece of DNA. A more recent advance in AAV vector technology has been the self-complementary (sc) vector, the genome of which is composed of complementary copies of the DNA insert linked in *cis* through a mutated AAV inverted terminal repeat (ITR). scAAV vectors have 10- to 100-fold higher transduction efficiency compared with traditional single-stranded AAV (ssAAV) vectors (McCarty *et al.*, 2001, 2003), facilitating more global applications, such as intravenous or intracerebrospinal fluid injection. However, a potential drawback of scAAV vectors for some genes is that the packaging capacity is cut in half, to approximately 2.2 kb of foreign DNA. Thus, a major challenge in effectively using scAAV vectors has been to combine minimal promoter, intron, and polyadenylation [poly(A)] elements in order to maximize the remaining space for the transgene-coding sequence (Wu *et al.*, 2008). To simplify our descriptions and discussion of the regulatory elements including the enhancer, promoter, and 5′ untranslated region (UTR), throughout this

[1]Gene Therapy Center, University of North Carolina, Chapel Hill, NC 27599.
[2]Department of Neurobiology, Duke University Medical Center, Durham, NC 27710.
[3]David H. Murdock Research Institute, Kannapolis, NC 28081.
[4]Department of Cell and Molecular Physiology, UNC Neuroscience Center, University of North Carolina, Chapel Hill, NC 27599.
[5]Bowles Center Alcohol Studies, University of North Carolina, Chapel Hill, NC 27599.
[6]Department of Psychiatry, University of North Carolina, Chapel Hill, NC 27599.
[7]Department of Pharmacology, University of North Carolina, Chapel Hill, NC 27599.

text these combined elements will often be referred to simply as the "promoter."

The cytomegalovirus (CMV) early enhancer/promoter and the hybrid CMV enhancer/chicken β-actin (CBA) promoter are commonly used in gene transfer studies with both therapeutic and reporter genes. These promoters are typically used to provide robust, long-term expression in all cell types. The 800-bp CMV enhancer/promoter has often been used to achieve rapid and ubiquitous expression, with the caveat that it is prone to silencing over time in some tissues, specifically the hippocampus, striatum, and substantia nigra in the brain (McCown *et al.*, 1996; Klein *et al.*, 1998; Paterna *et al.*, 2000; Tenenbaum *et al.*, 2004). Although promoters such as the neuron-specific enolase (NSE) and neuron-specific human platelet-derived growth factor-β (PDGF-β) chain can provide strong and long-term expression, their larger sizes make them less preferable for scAAV vectors. The 1.6-kb hybrid promoter composed of the CMV immediate-early enhance, CBA promoter, and CBA intron 1/exon 1 (commonly called the CAGGS promoter; Niwa *et al.*, 1991) has been shown to provide ubiquitous and long-term expression in the brain (Klein *et al.*, 2002). An 800-bp miniature version of this CMV enhancer/CBA promoter was made by replacing the CBA 5′ (UTR) with a smaller simian virus 40 (SV40) intron (Wang *et al.*, 2003). The smaller size of this promoter proved especially useful for scAAV vectors. However, we report that this shortened version of the CBA promoter does not support the same level of motor neuron (MN) gene expression as seen with the CMV promoter.

Given this difference, the following studies sought to determine whether the shortened CBA promoter contributed to this differential tropism and how one might overcome this limited cellular expression. We found that the mini-CBA promoter was deficient for MN expression and that the CMV promoter, although giving robust initial MN expression, was silenced by 10 weeks in the spinal cord. Our studies resulted in the development of a novel version of the CBA promoter, called CBh, which provides long-term transgene expression in all cell types seen with the CBA or CMV promoter, at levels matching or exceeding each. In a separate effort to develop a smaller neural promoter to aid in packaging larger transgenes at lower regulated expression levels, we tested a truncated 229-bp promoter fragment from the murine methyl-CpG-binding protein-2 (MeCP2) gene that can drive neuronal expression. As a result of these studies, two novel promoters are now available to drive long-term neural expression: one with strong ubiquitous expression and one with an advantageous smaller size and weak neuronal expression.

Materials and Methods

Vector constructs

All vectors used enhanced green fluorescent protein (GFP) as the packaged gene. The sources of enhancer, promoter, intron, and polyadenylation signal are provided in Table 1.

Recombinant AAV production

Recombinant AAV (rAAV) vectors used the AAV serotype 9 capsid and were produced by a triple-transfection method in human embryonic kidney 293 (HEK293) cells as described (Grieger *et al.*, 2006). All recombinant vectors packaged self-complementary genomes with enhanced GFP. Highly pure recombinant virus containing self-complementary genomes was recovered by passage through two sequential CsCl gradients, and then the peak fractions were dialyzed in phosphate-buffered saline (PBS) containing 5% D-sorbitol. Viral titers were determined by quantitative polymerase chain reaction (qPCR) (Gray *et al.*, 2010).

Analysis of promoters in cultured rat hippocampal slices

Rat hippocampal slices were prepared as described by Fuller and Dailey (2007). Briefly, postnatal day 5 (P5) Sprague-Dawley rat pups were killed and the hippocampi were manually dissected. Harvested tissue was sliced into 250-μm-thick sections, using a McIlwain tissue chopper, and plated on PICM0RG50 0.4-μm membranes (Millipore, Bedford, MA) with full complement medium. Slices were cultured for 7 days before infection. Each viral vector was diluted to 1×10^7 vector genomes (VG)/μl in PBS and individual slices were infected with approximately 5 μl (5×10^7 VG) by direct application. Slices were incubated in 5% CO_2 at 37°C and imaged daily. Average fluorescence intensity from each slice was measured with a stereomicroscope (Lumar; Carl Zeiss, Oberkochen, Germany) with a 0.5 numerical aperture (NA) objective. The observed fluorescence was normalized to a control test strip (available upon request from Chroma Technology, Bellows Falls, VT). In addition, each image was scaled on the basis of exposure time, and detector linearity was measured each day. High-resolution images were obtained by two-photon non-descan detection microscopy on a Zeiss Axio Examiner with 710 confocal scanning unit. All images were recorded with either a $\times$20 Apochromat 1.0 NA or $\times$63 Plan-Apochromat 0.8 NA lens set for Nyquist sampling with a non-descan photomultiplier tube detector.

To evaluate GFP levels per cell (see Fig. 2), high-resolution images of hippocampal neurons in organotypic configuration were examined. The images were collected as a three-dimensional data set, and individual cells were manually selected by outlining the area for a cell on each plane within the z stack. The total intensity and thresholded area were calculated at each plane and summated to provide the total integrated intensity and summated area, respectively. Cell size is directly related to the summated area for the individual cell across the entire z stack. The integrated intensity/summated area is directly related to the GFP concentration. For data presentation (see Fig. 2), cells were sorted into exponentially larger bins based on cell size. Here we set a threshold that all bins must contain three individual cells to be considered significant and included in Fig. 2.

Rodent injections

All investigations were approved by the University of North Carolina (UNC)-Chapel Hill Institutional Animal Care and Use Committee (Chapel Hill, NC). All injections were done in 8- to 12-week-old female BALB/c mice weighing approximately 20 g, purchased from Jackson Laboratory (Bar Harbor, ME). For intravenous delivery, 200 μl of scAAV9 vector (2×10^{11} total VG) was injected into the tail vein. Four or 14 weeks after vector injection, each mouse was killed and

Table 1. Constructs Packaged in AAV

Construct	*Enhancer*	*Promoter*	*Intron*	*Poly(A)*
CMV-GFP	CMV early[a]	CMV early[b]	Chimeric hβ-Globin[c]/mIgG[d]	SV40 early[e]
CBA-GFP	CMV early[a]	chβ-Actin[f]	Truncated SV40 late 16S[g]	BGH[h]
CBh-GFP	CMV early[a]	chβ-Actin[f]	Chimeric chβ-Actin[i]/MVM[j]	BGH[h]
MeP-GFP	NA	mMeCP2[k]	NA	Synthetic[l]

NA, not applicable; for other abbreviations see text.
[a]GenBank accession no. NC_006273.2, nt 175625–175294.
[b]GenBank accession no. NC_006273.2, nt 175043–175294.
[c]GenBank accession no. AC_000054.1, nt 5366740–5366826.
[d]GenBank accession no. L26879.1, nt 678–705.
[e]GenBank accession no. NC_001669.1, nt 2548–2774.
[f]GenBank accession no. X00182.1, nt 280–540.
[g]GenBank accession no. NC_001669.1, nt 502–561, 1410–1497.
[h]Bovine growth hormone, GenBank accession no. EF592533.1, nt 1827–2034.
[i]GenBank accession no. X00182.1, nt 544–676.
[j]GenBank accession no. NC_001510.1, nt 2312–2403 (VP intron).
[k]See Adachi *et al.* (2005), nt −170 to +53 from mapped transcription start.
[l]Synthetic, based on Levitt *et al.* (1989).

transcardially perfused with PBS containing heparin at 1 U/ml (Abraxis Pharmaceutical Products, Schaumburg, IL).

For intrathecal delivery, 3.75 μl of scAAV9 vector (1.25×10^9 total VG) was mixed with 1.25 μl of 60% lidocaine (MPI Biomedicals, Solon, OH) in PBS, to make a vector solution containing 15% lidocaine in 1× PBS plus 3.75% sorbitol. This 5-μl solution was then injected into the intrathecal space of the lower lumbar cord of a nonsedated mouse, as described in Hylden and Wilcox (1980). Needle penetration into the intrathecal space was indicated by a tail flick, and then successful injections were confirmed by transient (10–15 min) bilateral paralysis of the hind limbs, from the lidocaine. Mice were killed 3 or 10 weeks later, and then transcardially perfused with PBS.

Tissue processing, immunohistochemistry, and immunofluorescence

For all immunohistochemistry, samples were processed as follows. After 48 hr of fixation in freshly made PBS with 4% paraformaldehyde, the entire brain and lumbar spinal cord were sectioned at 40 μm, using a vibratome (Leica Microsystems, Wetzlar, Germany) at room temperature. To enhance the signal observed with GFP, every fifth section was processed for immunohistochemistry (IHC). Samples were incubated for 1 hr with shaking at room temperature in blocking solution (10% goat serum, 0.1% Triton X-100, 1× PBS), and then incubated for 48–72 hr at 4°C in primary antibody solution (3% goat serum, 0.1% Triton X-100, 1× PBS, rabbit anti-GFP [AB3080, diluted 1:500; Millipore]). After washing three times in 1× PBS, secondary amplification was performed with a VECTASTAIN Elite ABC kit (#PK-6101; Vector Laboratories) with 3,3′-diaminobenzidine tetrahydrochloride (DAB) (04008; Polysciences, Warrington, PA) substrate and nickel–cobalt intensification of the reaction product.

For the MeCP2 promoter (MeP)–GFP colocalization studies, blocking and primary antibody incubations were done as described previously, except that donkey serum was used for choline acetyltransferase (ChAT) labeling. After washing, the sections were incubated with shaking for 1 hr at room temperature in secondary antibody solution (3% goat or donkey serum, 0.1% Triton X-100, 1× PBS, secondary antibodies), and then washed three more times in 1× PBS. Primary antibodies were as follows: rabbit anti-GFP (AB3080, diluted 1:500; Millipore) with either mouse anti-neuron-specific nuclear protein (NeuN) (MAB377, diluted 1:500; Millipore) or goat anti-ChAT (AB144P, diluted 1:100; Millipore). Secondary antibodies were as appropriate, each at 1:1000 dilution: goat anti-rabbit Alexa 488 (A11008; Invitrogen, Carlsbad, CA), Alexa Fluor 594-conjugated goat anti-mouse (A11032; Invitrogen), and Alexa Fluor 594-conjugated donkey anti-goat (A11058; Invitrogen). Confocal imaging was performed at the Michael Hooker Microscopy Center at UNC-Chapel Hill, using a Zeiss Axiovert LSM 510 laser confocal microscope. Images were processed with Zeiss LSM Image Browser software. Dual-label immunofluorescence images were reconstructed from at least five consecutive steps in a *z* series taken at 1.3-μm intervals through the section of interest, using a ×20 objective.

To examine MeP-mediated GFP expression in peripheral organs, samples were prepared as for IHC described previously (48 hr of paraformaldehyde fixation, 40-μm vibratome sections), and incubated with or without rabbit anti-GFP as done for IHC brain samples. Both sets of tissue sections were then incubated with Alexa Fluor 488-conjugated goat anti-rabbit (A11008; Invitrogen), and then washed and mounted to slides. GFP fluorescence was visualized with a Leica DM IRB wide-field fluorescence microscope, using a ×20 objective.

For studies regarding the dorsal root ganglia (DRG) after intrathecal injection, lumbar levels L2 to L6 were removed from each animal and immersion-fixed for 4 hr in cold 4% paraformaldehyde in 0.1 *M* phosphate buffer, pH 7.4. After cryoprotection in 30% sucrose in 0.1 *M* phosphate buffer, ganglia were sectioned at a thickness of 20 μm and collected on SuperFrost Plus slides. Every fourth section was incubated overnight with a cocktail containing a chicken IgY to GFP (GFP-1020, diluted 1:600; Aves Labs, Tigard, OR) and a rabbit IgG to substance P (20064, diluted 1:600; ImmunoStar, Hudson, WI). After several buffer rinses, slides were incubated for 3 hr with a mixture containing a goat anti-chicken IgY coupled to Alexa Fluor 488 (A11039, diluted 1:200; Invitrogen), a goat anti-rabbit IgG coupled to Alexa Fluor 633

(A21070, diluted 1:200; Invitrogen), and isolectin GS-IB_4 coupled to Alexa Fluor 568 (I21412, diluted 1:100; Invitrogen). After rinses, slides were coverslipped with Fluoro-Gel (17985-10; Electron Microscopy Sciences, Hatfield, PA). Images were obtained with the UNC Neuroscience Center's Zeiss LSM 510 laser confocal microscope and collected as maximal projections.

Results

Construction of a modified mini-CBA promoter, termed CBh

Discrepancies in the literature (Duque *et al.*, 2009; Foust *et al.*, 2009), our own preliminary observations, and those of our colleagues (Snyder *et al.*, 2011), suggested that the miniature CBA promoter expressed poorly in MNs. The miniature CBA promoter has reduced expression relative to the full-length CAGGS promoter (data not shown), so we hypothesized that when the β-actin 5′ UTR in the CAGGS promoter was replaced with the truncated SV40 intron, this resulted in reduced MN expression specifically, in addition to the overall reduced expression. To test whether a better version of the CBA promoter could be made, we replaced this intron with another sequence to produce an 800-bp modified CBA promoter with the potential for ubiquitous expression in the CNS. The minute virus of mice (MVM) VP intron was previously shown to provide enhanced liver expression compared with a panel of other small introns (Wu *et al.*, 2008), and therefore it served as an initial candidate to replace the truncated SV40 intron. The construct resulting from these studies replaced the SV40 intron in the CBA promoter with a hybrid intron composed of a 5′ donor splice site from the chicken β-actin 5′ UTR and a 3′ acceptor splice site from MVM. This new version of the chicken β-actin "promoter" (enhancer, promoter, and 5′ UTR) was termed "CBh" for CBA hybrid intron (for construct compositions, see Table 1).

CMV, CBA, and CBh promoters show different expression kinetics and cell-type specificity in cultured rat hippocampal slices

To define a time course of early CNS expression comparing the CMV, CBA, and CBh promoters, an *ex vivo* assay was used to compare these AAV vectors in the rat hippocampus. Rat hippocampal organotypic slices were infected with AAV9 vectors using a CMV, CBA, or CBh promoter driving the expression of GFP. Promoter efficacy was monitored by evaluating GFP production daily over a 5-day time course. All three promoters demonstrated weak fluorescence 24 hr after infection (Fig. 1P; signal-to-background ratio, 2:1). The CMV and CBh promoters provided a significant increase in fluorescence 48 hr after infection, and the CBA promoter was less effective at the equivalent time point (Fig. 1). Over the next 72 hr the CMV and CBh promoters demonstrated equivalent GFP expression, whereas the CBA promoter system was at a consistently lower level (Fig. 1). High-resolution images were collected on day 5 after infection to ascertain cell specificity of expression for each promoter. These data indicate that all three promoters (CMV, CBh, and CBA) did not demonstrate any selectivity for cellular subtypes within the hippocampus (data not shown). To gain better resolution of individual cell morphology and to assess relative GFP concentration in individual cells, a 1:100 dilution of vector was applied to hippocampal organotypic slices and visualized for GFP expression after 5 days. Individual cells with each promoter treatment were randomly selected and the total GFP fluorescence intensity was plotted against the total three-dimensional area for each cell (Fig. 2A). By binning the cells according to size, the relative GFP concentration could be assessed in different cell types in an unbiased fashion, and for each promoter there was no more than a 2-fold variation in GFP concentration among bins of different sizes. These data indicate that the CBA, CMV, and CBh promoters express GFP at homogeneous levels within different cell types of the hippocampus. This analysis also recapitulated the findings in Fig. 1, that is, that the CBA promoter expresses at consistently lower levels than the CMV or CBh promoter. No apparent differences in cell specificity were observed by visual inspection, although the intensity of GFP expression was reduced in CBA compared with CMV and CBh (Fig. 2B–D).

CMV, CBA, and CBh promoters differ in their in vivo *cell-specific expression profiles*

To compare the CMV, CBA, and CBh promoters for cell type-specific expression in the CNS *in vivo*, mice received a tail vein injection of scAAV9/GFP vector (2×10^{11} VG), using each of the promoters to drive GFP expression. Four weeks later the mice were killed, and sections of the brain and spinal cord were assessed for GFP expression. We observed neuronal and glial expression throughout the CNS with all promoters, but the cell-specific expression and intensity of expression differed, in some cases substantially, on the basis of which promoter was used (Fig. 3). Compared with the CBA and CBh promoters, the CMV promoter showed reduced expression in hippocampal neurons 4 weeks postinjection, consistent with observations made by McCown and colleagues and Klein and colleagues that the CMV promoter is silenced over time in the hippocampus after direct intracranial injection (McCown *et al.*, 1996; Klein *et al.*, 1998). In the striatum, however, neuronal expression from the CMV, CBA, and CBh promoters was equivalent. In general, throughout the entire CNS, stronger GFP expression in astrocytes was observed with the CBA and CBh promoters than with the CMV promoter. A striking difference was seen in the ventral horn of the spinal cord. The CBA promoter showed a small number of GFP-positive cells with neuronal morphology, approximately two to four per 40-μm slice at this dose. In contrast, the same dose of vector using the CMV promoter resulted in 30–40 GFP-positive neuron-like cells per 40-μm slice. The CBh promoter also provided a large number of GFP-positive neuron-like cells, similar to that observed with the CMV promoter, but an accurate count was obscured by the large number of strongly GFP-positive astrocytes. On the basis of their morphology, large size, and location in the ventral horn, most of these neurons appeared to be motor neurons (MNs).

The CMV promoter becomes silenced in spinal cord MNs and DRG, but the CBh promoter provides robust, long-term expression in these cells

To specifically investigate short- and long-term expression in MNs and dorsal root ganglia (DRG) with the CBA, CMV,

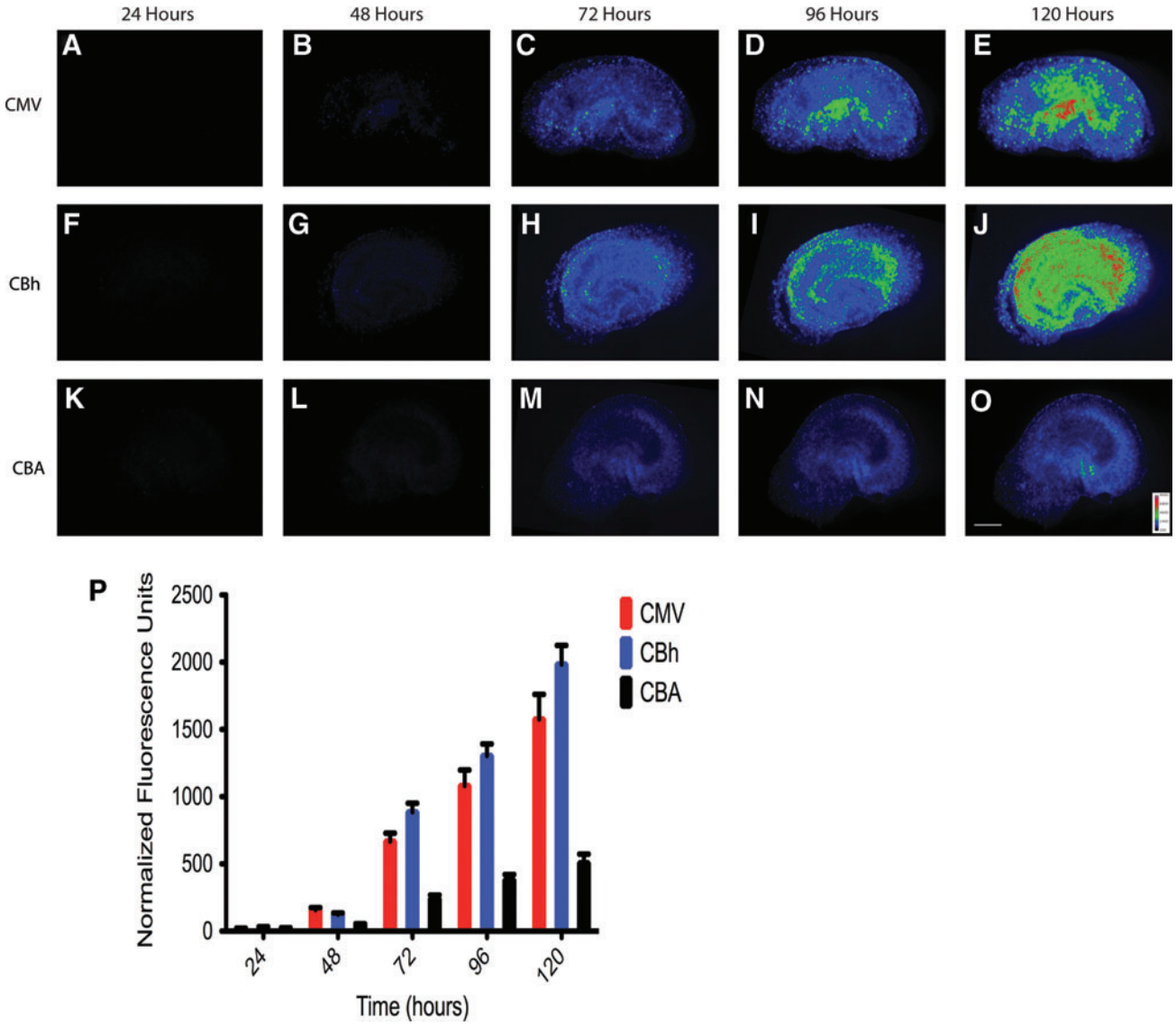

FIG. 1. CMV, CBh, and CBA promoters demonstrate distinct kinetics in cultured rat hippocampal slices. Rat hippocampal slices were infected with 5×10^7 VG after 7 days in culture, and GFP expression was monitored for 5 days. The time course of GFP expression was examined for the CMV **(A–E)**, CBh **(F–J)**, and CBA **(K–O)** promoters at five time points. All images are mapped to the pseudo-color gray wedge depicted in **(O)**. All images are set to equivalent scales with the scale bar in **(O)** set to 600 μm. All three promoters demonstrated observable fluorescence 24 hr after infection and steadily increased during the 5-day time course **(P)**. The fluorescence intensity for each measurement was normalized to a fluorescent test strip recorded each day. The values are scaled to account for exposure time required for each image. *Note:* The exposure times were adjusted to ensure all images were acquired within the dynamic range of the detector, and the detector linearity was evaluate each day for the entire time course **(P)**. Color images available online at www.liebertonline.com/hum

and CBh promoters, we delivered scAAV9/GFP vectors intrathecally in mice. In the ventral horn of the lumbar spinal cord, mice killed 3 weeks postinjection showed a cell-type bias similar to that seen with intravenous vector administration. CMV expression was detected mostly in cells with neuronal morphology, CBA expression was detected mostly in cells with glial morphology, and CBh expression could be detected in both cell types (Fig. 4, row A). In the DRG, expression was observed in multiple cell types with all three promoters (Fig. 4, row C). At 10 weeks postinjection in the spinal cord and DRG, expression of GFP with the scAAV9/CMV vectors was significantly reduced, but the scAAV9/CBh vectors showed unchanged levels of expression (Fig. 4, rows B and D).

Within the CNS, the 229-bp murine MeCP2 promoter preferentially expresses in neurons in vivo

The CMV and miniature CBA enhancer/promoters are each approximately 800 bp long, making them amenable for high expression in scAAV vectors, which have a packaging constraint of approximately 2.2 kb of foreign DNA. Smaller neural promoters would have an advantage for certain CNS applications, when a larger transgene must be packed in

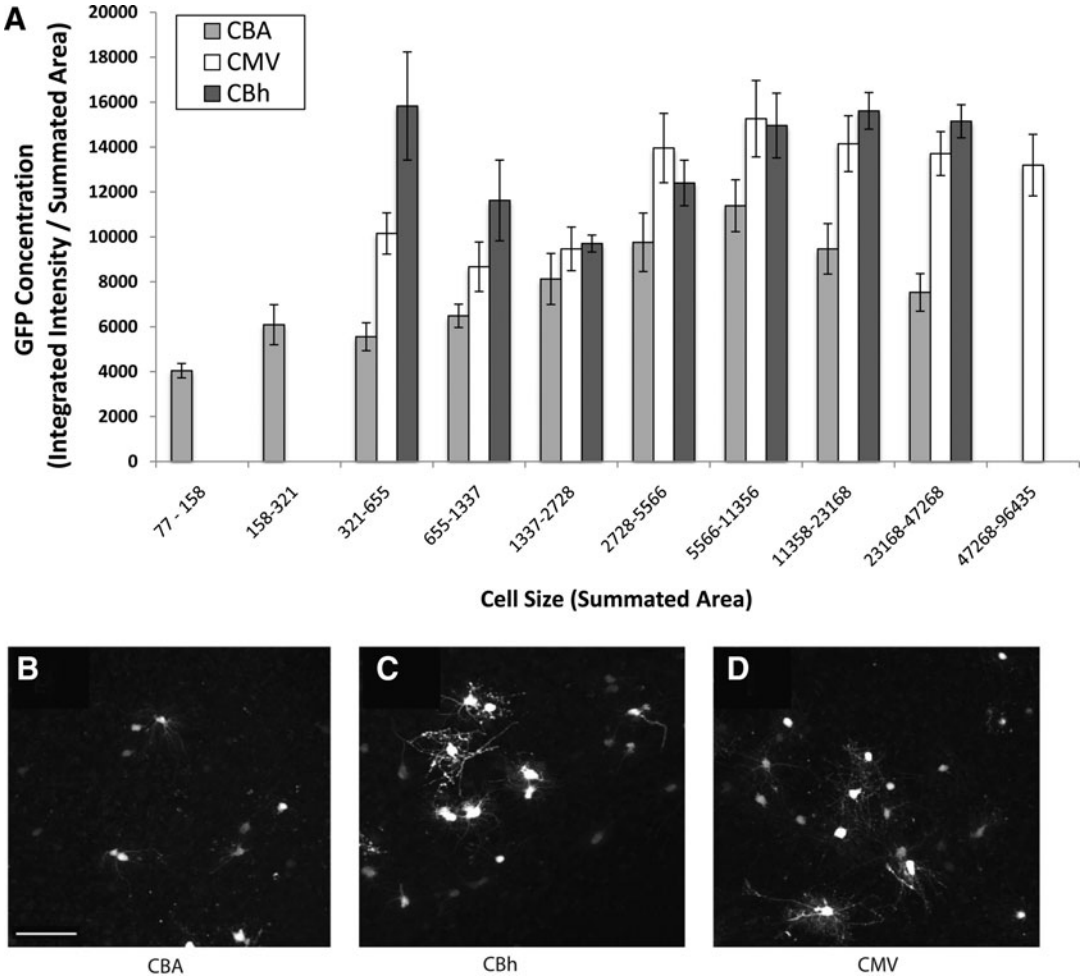

FIG. 2. GFP expression remains constant independent of cell size, and the CMV, CBA, and CBh promoters express in a broad range of cells. Rat hippocampal slices were infected with 5×10^5 VG after 7 days in culture, and GFP expression was monitored after 5 days. **(A)** Cell size was measured by summating the area for each cell throughout the three-dimensional data set. Individual cells were outlined manually, and the total intensity was measured for each plane. A relative GFP concentration was determined by dividing integrated intensity values by the summated area values. The individual cells were subsequently binned according to summated area to depict the size of these cells. Because of the large range of cell sizes, the individual bins increase in size based on an exponential scale. The CBA, CMV, and CBh promoters all demonstrate a homogeneous GFP concentration independent of the size of the cell. **(B–D)** Images are *z*-stack maximal projections of native GFP fluorescence. Representative images of greater than 10 fields are shown. **(B)** CBA, **(C)** CBh, **(D)** CMV. Scale bar (100 μm) is shown in **(B)**.

scAAV vectors. A promoter fragment from the murine MeCP2 gene has been characterized as having primarily neuronal expression, although low expression has also been documented in glial cells (Adachi *et al.*, 2005; Rastegar *et al.*, 2009). On the basis of the studies by Adachi and colleagues, we hypothesized that the core components of the murine MeCP2 promoter (MeP) were contained in a 229-bp fragment. An AAV construct was created to use this 229-bp fragment to drive GFP expression. A 49-bp synthetic poly(A) signal (Levitt *et al.*, 1989) was also used, providing approximately 1.9 kb of space to package a foreign gene in place of GFP in scAAV. Transfection of constructs using this promoter in HEK293 cells showed low expression relative to the CBA and CMV promoters, indicating some potential for low nonneuronal expression (data not shown). When packaged into scAAV and injected intravenously into mice, the MeP promoter provided neuron-specific gene expression in the CNS (Fig. 5). Visualization of expression by native fluorescence was not readily apparent (data not shown), but positive cells were apparent by IHC and immunofluorescence (IF), all with neuronal morphology. Co-IF with NeuN in the hippocampus confirmed that positive cells were neurons, and expression in spinal cord MNs was identified by colabeling with ChAT (Fig. 5). An identical expression profile with the MeP promoter was observed at 14 weeks postinjection, indicating that MeP provides long-term expression (Fig. 6). At 14 weeks postinjection, expression was also seen in the liver, heart, and kidney, but not the spleen, indicating that the promoter is not neuron specific outside of the CNS (Fig. 7).

Discussion

Consistent with published reports (McCown *et al.*, 1996; Klein *et al.*, 1998; Paterna *et al.*, 2000; Tenenbaum *et al.*, 2004), we conclude from our results that AAV vectors using the

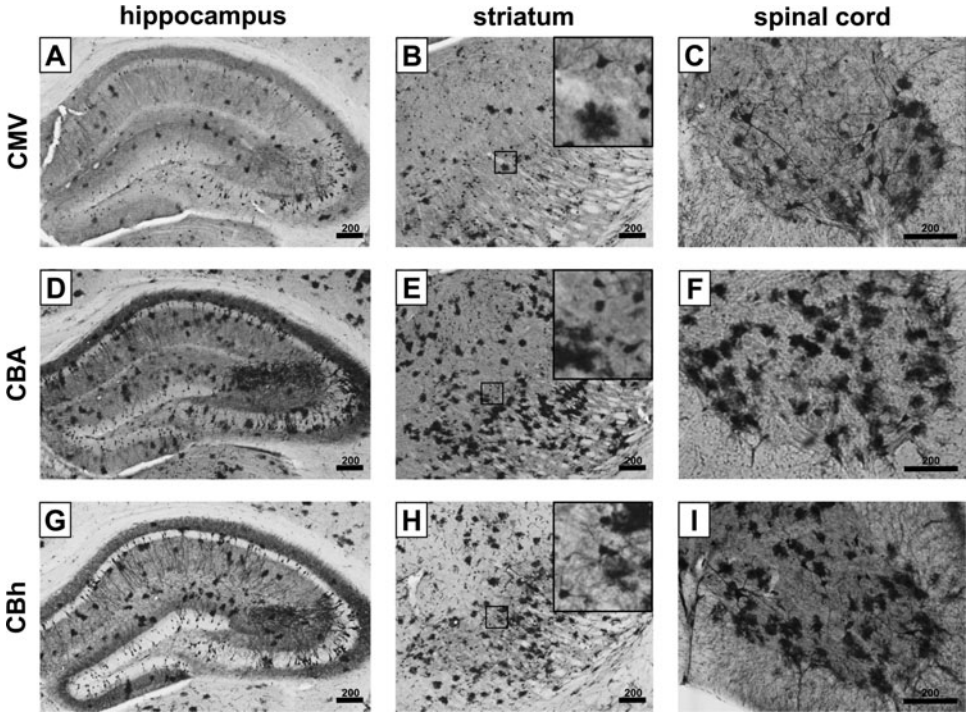

FIG. 3. *In vivo* expression of CMV, CBA, and CBh promoters. Adult mice were injected with equal titers of scAAV9/GFP under the control of the CMV **(A–C)**, CBA **(D–F)**, or CBh **(G–I)** promoter, and then were killed 4 weeks postinjection to assess GFP-positive cells. **(A)**, **(D)**, and **(G)** show the hippocampus (bregma, −2.0). **(B)**, **(E)**, and **(H)** show the striatum (bregma, −2.0), with the *insets* showing an additional ×5 magnification. **(C)**, **(F)**, and **(I)** show the ventral horn of the cervical spinal cord. Scale bars: 200 μm. All images are representative of at least three mice.

CMV promoter provide rapid and strong transgene expression that is prone to diminish significantly over time in certain cell types. The CBA promoter, for most CNS applications, provides ubiquitous expression in a wide variety of cells. Relative to the CMV promoter, however, the 800-bp CBA promoter used in our studies expressed poorly in MNs in the brainstem and spinal cord, resulting in an underestimate of the number of MNs targeted by AAV9. We genetically narrowed the cause for poor MN expression to the approximately 200-bp SV40 intron used to reduce the 1.6-kb CAGGS promoter to 800 bp, and functionally replaced it with a hybrid intron from the chicken β-actin intron 1 and MVM VP intron. In the context of the same AAV2 ITRs, CMV enhancer, CBA promoter, and bovine growth hormone (BGH) poly(A), the hybrid CBA/MVM intron supported expression in MNs comparable to the CMV promoter and significantly better than the CBA promoter with the SV40 intron. Moreover, the CBh promoter provided stronger expression in *ex vivo* rat hippocampal slices compared with CBA. Overall, our results indicate that the CBh promoter is a strong and ubiquitous promoter for CNS applications, equal to or better than the CMV or CBA promoter in these regards. It is important to clarify that our studies used the 800-bp miniature CBA promoter, and we would not extrapolate the findings of this study to the full-length 1.6-kb CBA (CAGGS; Niwa *et al.*, 1991) promoter. Moreover, the cell-specific expression patterns observed in these studies were influenced by the route of administration, because intraparenchymal brain injection of AAV9 leads to almost exclusive neuronal expression (Gray *et al.*, 2010).

Intravenous injection of scAAV9/GFP vectors leads to extensive AAV delivery to the brain and spinal cord (Duque *et al.*, 2009; Foust *et al.*, 2009). The differential promoter activity we observed in the spinal cord with CBA and CMV could explain the discrepancies in adult mouse MN transduction reported by Foust and colleagues and Duque and colleagues after intravenous injection (Duque *et al.*, 2009; Foust *et al.*, 2009). Foust and colleagues used the CBA promoter and reported only ~5% of MNs transduced at a dose of 1×10^{14} VG/kg. Duque and colleagues used the CMV promoter at the same dose and reported 5–19% of motor neurons (MNs) transduced in adult mice. Our results suggest that the higher percentage of MN transduction reported by Duque and colleagues could be a reflection of the promoter choice. Both reported strong MN expression when neonatal mice were injected, which suggests that the developmental stage also might influence promoter regulation. Furthermore, studies with other AAV serotypes might have underestimated the extent of potential transduction. For example, Vulchanova and colleagues tested intrathecal injections of AAV5 and AAV8 vectors using the CBA promoter, and reported extensive transduction of DRG but only minimal transduction of neurons in the spinal cord ventral horn (Vulchanova *et al.*, 2010).

When using scAAV vectors, which package only ~2.2 kb of foreign DNA, the choice of regulatory elements such as promoters and polyadenylation signals becomes limited. The CMV, miniature CBA, and CBh promoters described in this study are each approximately 800 bp, and with a 200-bp poly(A) sequence an scAAV vector will accommodate only approximately 1.2 kb of coding sequence. The neuron-specific synapsin and weak ubiquitous β-glucuronidase (GUSB) promoters are smaller alternatives at 480 and 378 bp, respectively (Shipley *et al.*, 1991; Kügler *et al.*, 2003; Husain *et al.*, 2009). The 229-bp murine MeCP2 promoter in these studies offers additional packaging space as well as long-term, weak, and neuron-specific expression. MeCP2 is a transcriptional regulator expressed primarily in neurons in the CNS, although it is also

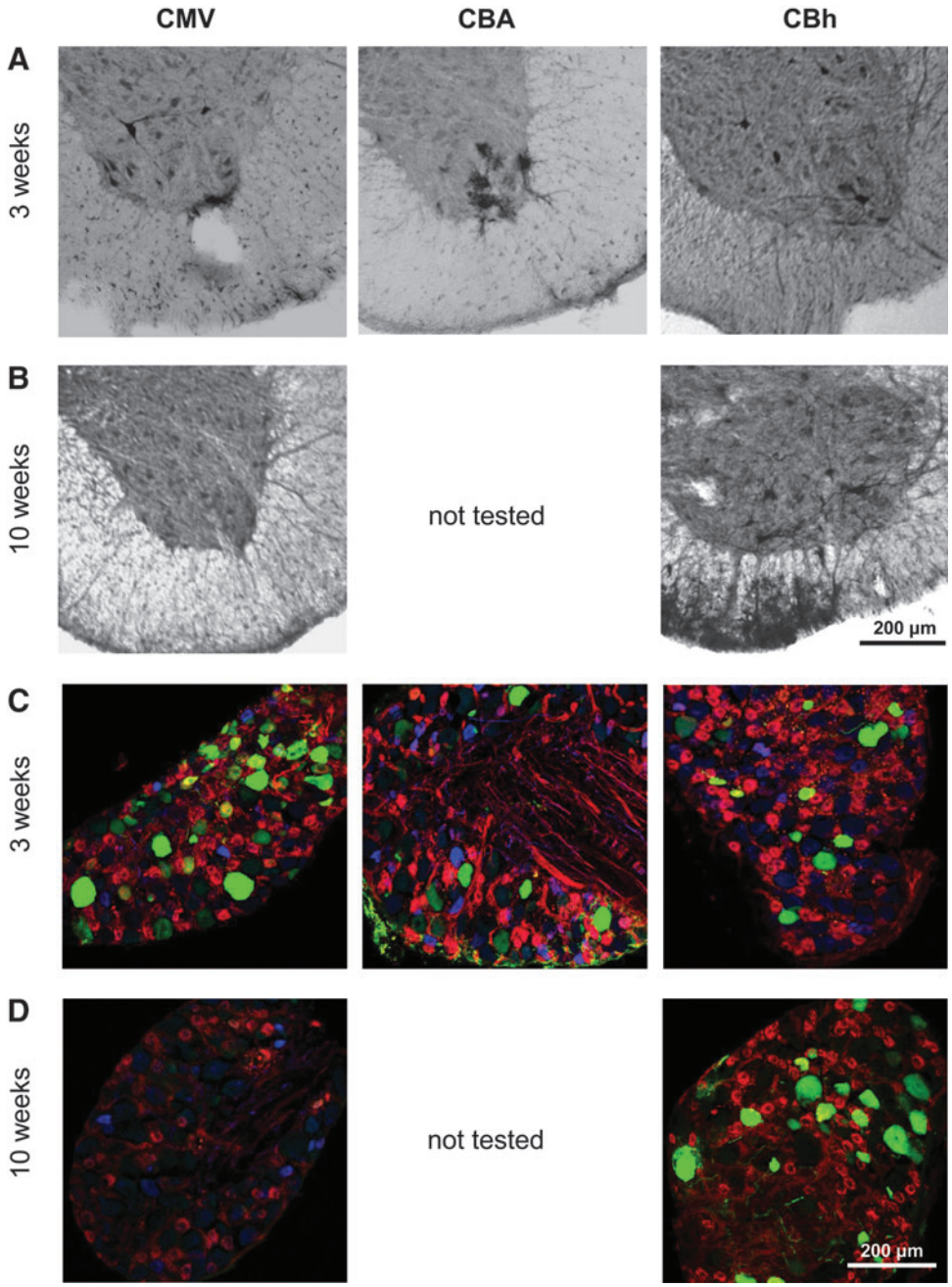

FIG. 4. Three- and 10-week expression profiles of the CBA, CMV, and CBh promoters in the spinal cord after intrathecal injection. Mice received a lumbar puncture injection of 1.25×10^{9} VG of scAAV9/GFP, and then they were killed 3 or 10 weeks postinjection to assess GFP-positive cells. Rows **A** and **B** illustrate spinal cords subjected to anti-GFP immunohistochemistry. Rows **C** and **D** show representative confocal coimmunofluorescence (co-IF) images using anti-GFP (green), anti-substance P (blue), and anti-GS-IB_4 (red). For each row, the *left* panel shows the CMV promoter, the *middle* panel shows the CBA promoter, and the *right* panel shows the CBh promoter. Row A, lumbar spinal cord at 3 weeks postinjection; row B, lumbar spinal cord at 10 weeks postinjection (CBA was not tested at this time point); row C, lumbar DRG at 3 weeks postinjection; row D, lumbar DRG at 10 weeks postinjection (CBA was not tested at this time point, and the 10-week CBh DRG image [*bottom right*] was not stained with anti-substance P). Scale bars: 200 μm. Images are representative of at least three mice for each variable.

ubiquitously expressed in other tissues (Shahbazian *et al.*, 2002). When incorporated into lentiviral vectors and tested *in vitro* and *ex vivo*, the full 700-bp MeCP2 promoter fragment expressed primarily in neurons with lower levels of expression also observed in astrocytes, as expected (Rastegar *et al.*, 2009). Although we could not detect expression of GFP outside of neurons in the CNS, expression of GFP was readily apparent in the liver, heart, and kidney. By using the 229-bp MeP promoter and a 49-bp synthetic poly(A) sequence (Levitt *et al.*, 1989), approxi-

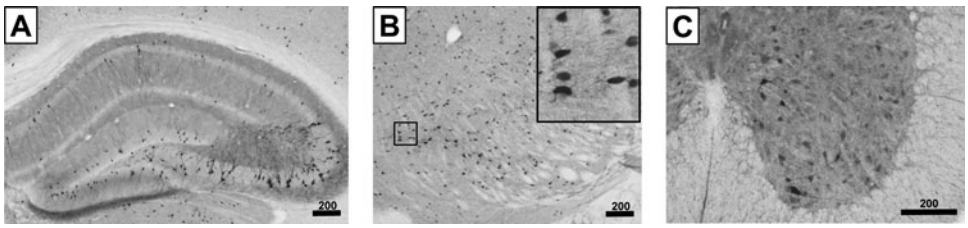

FIG. 5. *In vivo* expression of the MeP promoter at 4 weeks. Adult mice were injected intravenously with 2×10^{11} VG of scAAV9/MeP-GFP, and then killed 4 weeks postinjection to assess GFP-positive cells. **(A–C)** IHC using an anti-GFP antibody in the hippocampus **(A)**, striatum **(B)**, and spinal cord **(C)**. The *inset* in **(B)** shows an additional ×5 magnification. Representative confocal images showing co-IF with the indicated antibodies in the hippocampus and spinal cord are provided as Supplemental Figure 1. Scale bars: 200 μm.

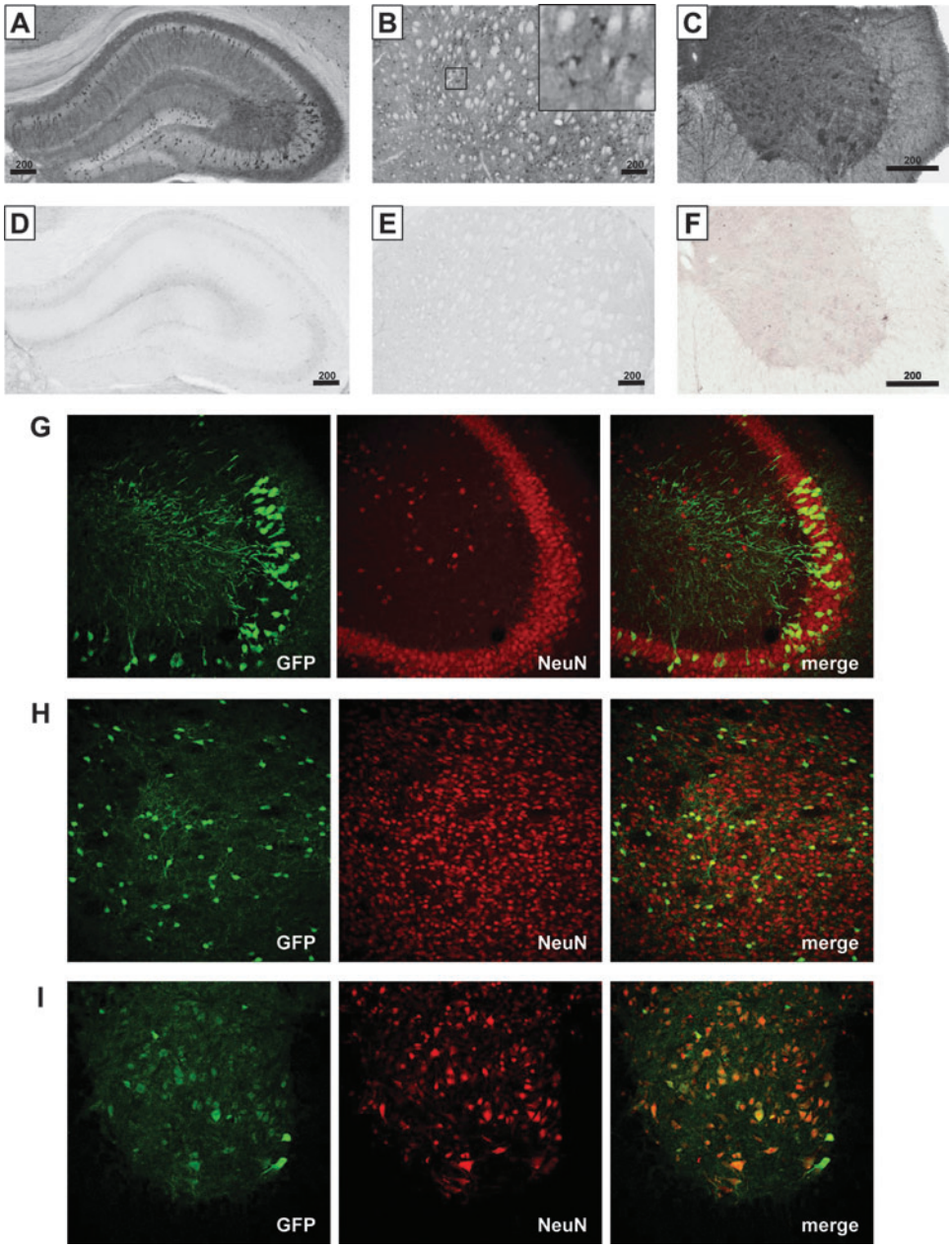

FIG. 6. *In vivo* expression of the MeP promoter at 14 weeks in the CNS. Adult mice were injected intravenously with 2×10^{11} VG of scAAV9/MeP-GFP, and then killed 14 weeks postinjection to assess GFP-positive cells in the CNS. **(A–C)** IHC using an anti-GFP antibody in the hippocampus **(A)**, striatum **(B)**, and spinal cord **(C)**. The *inset* in **(B)** shows an additional ×5 magnification. Rows **D–F** show alternate hippocampal **(D)**, striatal **(E)**, and spinal cord **(F)** sections prepared in parallel with no primary antibody. Rows **G–I** are representative confocal images showing co-IF with GFP and NeuN antibodies in the hippocampus, striatum, and spinal cord, respectively. Scale bars: 200 μm.

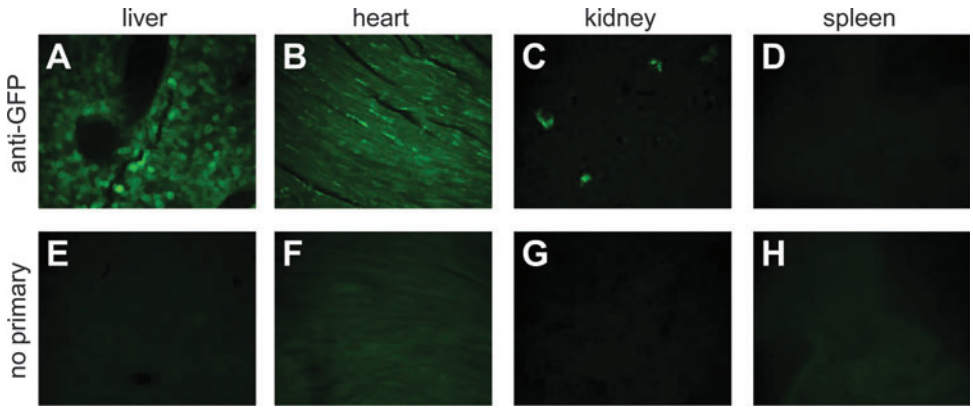

FIG. 7. *In vivo* expression of the MeP promoter at 14 weeks in peripheral organs. Adult mice shown in Fig. 6 were also assessed for GFP expression in the liver **(A** and **E)**, heart **(B** and **F)**, kidney **(C** and **G)**, and spleen **(D** and **H)**. Panels **A–D** show IF using an anti-GFP antibody, and panels **E–H** show neighboring sections prepared in parallel with no primary antibody. Color images available online at www.liebertonline.com/hum

mately 1.9 kb of genome capacity remained to package a transgene coding sequence in an scAAV vector. This extra packaging capacity could be critical for packaging therapeutic genes such as gigaxonin (1797 bp) for giant axonal neuropathy or tripeptidyl-peptidase I (1686 bp) for neuronal ceroid lipofuscinosis. Moreover, the low expression levels could be necessary when overexpression of the gene product could be deleterious, such as for Rett syndrome and fragile X syndrome (Peier *et al.*, 2000; Collins *et al.*, 2004).

In summary, these studies demonstrate potential confounders that can arise from variable promoter tropisms. We conclude that the 800-bp CBh promoter we developed is a ubiquitous promoter that is advantageous overall, relative to the CMV and CBA promoters, in terms of the range of cell types transduced, the strength of expression, and the duration of expression. We further report that the 229-bp MeP promoter fragment, when used in AAV vectors in the CNS, displays primarily low-level neuronal expression along with an advantageous small size.

Acknowledgments

This work was supported by generous grants from the ALS Association to R.J.S., the International Rett Syndrome Foundation to S.J.G., Hannah's Hope Fund to S.J.G., NINDS NS35633 to T.J.M., and grants to M.J.Z. from the NINDS (R01NS060725, R01NS067688). The authors thank Swati Yadav, Huijing Sun, and Isabella Bellon for technical assistance. The authors acknowledge Jim Wilson's group at the University of Pennsylvania for the discovery of AAV9, and thank Xiao Xiao at UNC and the UNC Vector Core for providing the AAV9 helper plasmid.

Author Disclosure Statement

The authors report no conflicts of interest.

References

Adachi, M., Keefer, E.W., and Jones, F.S. (2005). A segment of the Mecp2 promoter is sufficient to drive expression in neurons. Hum. Mol. Genet 14, 3709–3722.

Bessis, N., GarciaCozar, F.J., and Boissier, M.C. (2004). Immune responses to gene therapy vectors: Influence on vector function and effector mechanisms. Gene Ther. 11(Suppl. 1), S10–S17.

Collins, A.L., Levenson, J.M., Vilaythong, A.P., *et al.* (2004). Mild overexpression of MeCP2 causes a progressive neurological disorder in mice. Hum. Mol. Genet 13, 2679–2689.

Duque, S., Joussemet, B., Riviere, C., *et al.* (2009). Intravenous administration of self-complementary AAV9 enables transgene delivery to adult motor neurons. Mol. Ther. 17, 1187–1196.

Foust, K.D., Nurre, E., Montgomery, C.L., *et al.* (2009). Intravascular AAV9 preferentially targets neonatal neurons and adult astrocytes. Nat. Biotechnol. 27, 59–65.

Fuller, L., and Dailey, M.E. (2007). Preparation of rodent hippocampal slice cultures. CSH Protoc. doi:10.1101/pdb.prot4848.

Goncalves, M.A. (2005). Adeno-associated virus: From defective virus to effective vector. Virol. J. 2, 43.

Gray, S.J., Blake, B.L., Criswell, H.E., *et al.* (2010). Directed evolution of a novel adeno-associated virus (AAV) vector that crosses the seizure-compromised blood–brain barrier (BBB). Mol. Ther. 18, 570–578.

Grieger, J.C., Choi, V.W., and Samulski, R.J. (2006). Production and characterization of adeno-associated viral vectors. Nat. Protoc 1, 1412–1428.

Haberman, R.P., McCown, T.J., and Samulski, R.J. (1998). Inducible long-term gene expression in brain with adeno-associated virus gene transfer. Gene Ther. 5, 1604–1611.

Husain, T., Passini, M.A., Parente, M.K., *et al.* (2009). Long-term AAV vector gene and protein expression in mouse brain from a small pan-cellular promoter is similar to neural cell promoters. Gene Ther. 16, 927–932.

Hylden, J.L., and Wilcox, G.L. (1980). Intrathecal morphine in mice: A new technique. Eur. J. Pharmacol. 67, 313–316.

Klein, R.L., Meyer, E.M., Peel, A.L., *et al.* (1998). Neuron-specific transduction in the rat septohippocampal or nigrostriatal pathway by recombinant adeno-associated virus vectors. Exp. Neurol. 150, 183–194.

Klein, R.L., Hamby, M.E., Gong, Y., *et al.* (2002). Dose and promoter effects of adeno-associated viral vector for green fluorescent protein expression in the rat brain. Exp. Neurol. 176, 66–74.

Kügler, S., Lingor, P., Schöll, U., *et al.* (2003). Differential transgene expression in brain cells *in vivo* and *in vitro* from AAV-2 vectors with small transcriptional control units. Virology 311, 89–95.

Levitt, N., Briggs, D., Gil, A., and Proudfoot, N.J. (1989). Definition of an efficient synthetic poly(A) site. Genes Dev. 3, 1019–1025.

McCarty, D.M., Monahan, P.E., and Samulski, R.J. (2001). Self-complementary recombinant adeno-associated virus (scAAV) vectors promote efficient transduction independently of DNA synthesis. Gene Ther. 8, 1248–1254.

McCarty, D.M., Fu, H., Monahan, P.E., *et al.* (2003). Adeno-associated virus terminal repeat (TR) mutant generates self-complementary vectors to overcome the rate-limiting step to transduction *in vivo*. Gene Ther. 10, 2112–2118.

McCown, T.J., Xiao, X., Li, J., *et al.* (1996). Differential and persistent expression patterns of CNS gene transfer by an adeno-associated virus (AAV) vector. Brain Res. 713, 99–107.

Niwa, H., Yamamura, K., and Miyazaki, J. (1991). Efficient selection for high-expression transfectants with a novel eukaryotic vector. Gene 108, 193–199.

Paterna, J.C., Moccetti, T., Mura, A., *et al.* (2000). Influence of promoter and WHV post-transcriptional regulatory element on AAV-mediated transgene expression in the rat brain. Gene Ther. 7, 1304–1311.

Peier, A.M., McIlwain, K.L., Kenneson, A., *et al.* (2000). (Over)correction of FMR1 deficiency with YAC transgenics: Behavioral and physical features. Hum. Mol. Genet. 9, 1145–1159.

Rastegar, M., Hotta, A., Pasceri, P., *et al.* (2009). MECP2 isoform-specific vectors with regulated expression for Rett syndrome gene therapy. PLoS One 4, e6810.

Shahbazian, M.D., Antalffy, B., Armstrong, D.L., and Zoghbi, H.Y. (2002). Insight into Rett syndrome: MeCP2 levels display tissue- and cell-specific differences and correlate with neuronal maturation. Hum. Mol. Genet 11, 115–124.

Shipley, J.M., Miller, R.D., Wu, B.M., *et al.* (1991). Analysis of the 5′ flanking region of the human β-glucuronidase gene. Genomics 10, 1009–1018.

Snyder, B.R., Gray, S.J., Quach, E.T., *et al.* (2011). Comparison of adeno-associated viral vector serotypes for spinal cord and motor neuron gene delivery. Hum. Gene Ther. (in press).

Tenenbaum, L., Chtarto, A., Lehtonen, E., *et al.* (2004). Recombinant AAV-mediated gene delivery to the central nervous system. J. Gene Med. 6(Suppl. 1), S212–S222.

Vulchanova, L., Schuster, D.J., Belur, L.R., *et al.* (2010). Differential adeno-associated virus mediated gene transfer to sensory neurons following intrathecal delivery by direct lumbar puncture. Mol. Pain 6, 31.

Wang, Z., Ma, H.I., Li, J., *et al.* (2003). Rapid and highly efficient transduction by double-stranded adeno-associated virus vectors *in vitro* and *in vivo*. Gene Ther. 10, 2105–2111.

Wu, Z., Sun, J., Zhang, T., *et al.* (2008). Optimization of self-complementary AAV vectors for liver-directed expression results in sustained correction of hemophilia B at low vector dose. Mol. Ther. 16, 280–289.

Address correspondence to:
Dr. R. Jude Samulski
UNC Gene Therapy Center
7119 Thurston Bowles, CB 7352
Chapel Hill, NC 27599-7352

E-mail: rjs@med.unc.edu

Received for publication December 22, 2010;
accepted after revision April 8, 2011.

Published online: April 8, 2011.